Branka Vulesevic,[1,2] Brian McNeill,[1] Ferdinando Giacco,[3] Kay Maeda,[1]
Nick J.R. Blackburn,[1,2] Michael Brownlee,[3] Ross W. Milne,[4] and Erik J. Suuronen[1,2]

Methylglyoxal-Induced Endothelial Cell Loss and Inflammation Contribute to the Development of Diabetic Cardiomyopathy

Diabetes 2016;65:1699–1713 | DOI: 10.2337/db15-0568

The mechanisms for the development of diabetic cardiomyopathy remain largely unknown. Methylglyoxal (MG) can accumulate and promote inflammation and vascular damage in diabetes. We examined if overexpression of the MG-metabolizing enzyme glyoxalase 1 (GLO1) in macrophages and the vasculature could reduce MG-induced inflammation and prevent ventricular dysfunction in diabetes. Hyperglycemia increased circulating inflammatory markers in wild-type (WT) but not in GLO1-overexpressing mice. Endothelial cell number was reduced in WT-diabetic hearts compared with nondiabetic controls, whereas GLO1 overexpression preserved capillary density. Neuregulin production, endothelial nitric oxide synthase dimerization, and *Bcl-2* expression in endothelial cells was maintained in the hearts of GLO1-diabetic mice and corresponded to less myocardial cell death compared with the WT-diabetic group. Lower receptor for advanced glycation end products and tumor necrosis factor-α (TNF-α) levels were also observed in GLO1-diabetic versus WT-diabetic mice. Over a period of 8 weeks of hyperglycemia, GLO1 overexpression delayed and limited the loss of cardiac function. In vitro, MG and TNF-α were shown to synergize in promoting endothelial cell death, which was associated with increased angiopoietin 2 expression and reduced *Bcl-2* expression. These results suggest that MG in diabetes increases inflammation, leading to endothelial cell loss. This contributes to the development of diabetic cardiomyopathy and identifies MG-induced endothelial inflammation as a target for therapy.

In patients with type 2 and type 1 diabetes, cardiovascular complications are the main cause of morbidity and mortality. Although an increased incidence of atherosclerosis and coronary artery disease (CAD) is a primary reason for this, many patients suffer from clinically significant ventricular dysfunction even in the absence of these conditions. This ventricular dysfunction has been termed diabetic cardiomyopathy and is defined as myocardial left ventricular (LV) dysfunction independent of atherosclerosis and CAD (1). Diabetic cardiomyopathy is a major cause of heart failure in people with diabetes. Despite the lack of CAD, a strong association exists between diabetic cardiomyopathy and the presence of microvascular complications (2). For example, inflammation, endothelial dysfunction, abnormal vascular remodeling, and an impaired angiogenic response have all been linked to the myocardial apoptosis, fibrosis, and hypertrophy seen in diabetic cardiomyopathy (3), although the mechanisms involved have not been clearly defined.

The activation of endothelial cells (ECs) from a quiescent phenotype to a vasoconstrictive, proinflammatory, and proapoptotic state leads to the inability of the endothelium to properly function (4). In diabetes, ECs are directly exposed to excessive and/or fluctuating blood glucose levels, and hyperglycemia is a known contributing factor to the loss of endothelial function (5). This exposure can stimulate the generation of reactive oxygen species (ROS) and the production of toxic by-products of glycolysis, primarily methylglyoxal (MG), leading to the formation of advanced

[1]Division of Cardiac Surgery, University of Ottawa Heart Institute, Ottawa, Ontario, Canada
[2]Department of Cellular & Molecular Medicine, University of Ottawa, Ottawa, Ontario, Canada
[3]Diabetes Research Center, Departments of Internal Medicine and Pathology, Albert Einstein College of Medicine, Bronx, NY
[4]Diabetes and Atherosclerosis Laboratory, University of Ottawa Heart Institute, Ottawa, Ontario, Canada

Corresponding author: Erik J. Suuronen, esuuronen@ottawaheart.ca

Received 28 April 2015 and accepted 3 March 2016.

glycation end products (AGEs) (6). Under normal physiological conditions, MG is metabolized by the glyoxalase system, whereby glyoxalase 1 (GLO1), together with glyoxalase 2 and glutathione, reduce MG to D-lactate, thus preventing MG accumulation (7). In diabetes, the production of MG is accelerated while its detoxification is slowed (due to reduced GLO1 activity), leading to MG accumulation (8,9). Elevated MG levels have been shown to promote inflammatory responses that activate ECs and lead to EC dysfunction and vascular damage (10,11). In fact, MG alone can cause endothelial damage similar to that induced by high glucose (HG) (12–14).

The endothelium plays an important role in cardiomyocyte viability and function and in myocardial homeostasis (15,16). EC death can lead to repeated episodes of ischemia and myocardial infarction, the death of cardiomyocytes, and the development of ventricular dysfunction leading to heart failure (17). However, the link between MG-induced inflammation, EC damage, and cardiac function in diabetes remain unknown. The current study used mice that overexpress human GLO1 (hGLO1) in macrophages and the vasculature (18–20) to investigate the connection between increased vascular MG, the ensuing inflammation in ECs, and the development of ventricular dysfunction in the diabetic heart.

RESEARCH DESIGN AND METHODS

All studies were performed according to protocols approved by the University of Ottawa Animal Care Committee and in accordance with the National Institutes of Health *Guide for the Care and Use of Laboratory Animals*.

Animal Model

As described previously (18–20), C57BL/6 mice that overexpress hGLO1 were used. The cDNA encoding hGlo1 with an amino terminal c-myc epitope tag was cloned into the Not1-digested PEP8 plasmid, so that the hGlo1 insert was under the control of the murine preproendothelin promoter. Experiments were performed on 8- to 10-week-old male heterozygous GLO1 mice and their wild-type (WT) littermates. Mice were fed the Teklad Global 2019 Extruded Rodent Diet (Harlan) and kept in a 12/12 h light/dark cycle.

Induction of Diabetes Using Streptozotocin

Mice received an intraperitoneal injection of 50 mg/kg of streptozotocin (STZ) (Sigma-Aldrich) or vehicle only (citrate buffer control) for 5 consecutive days. Four groups of mice were generated: WT-control, GLO1-control, WT-diabetic, and GLO1-diabetic. Fasting blood glucose measurements were taken 7 days after the last STZ injection and again after the animals were killed. Mice with glucose levels above 15 mmol/L at the beginning of the study were considered hyperglycemic (diabetic). Both diabetic groups had increased fasting blood glucose levels at the end of the study (~20 mmol/L), with no significant difference between them (Table 2).

Serum Analysis

ELISA assay kits (RayBiotech, Inc.) were used to measure blood serum levels of markers for endothelial inflammation (soluble intercellular adhesion molecule 1 [ICAM-1], vascular cell adhesion molecule 1 [VCAM-1], and E-selectin, presented as pg/mL of serum) at 8 weeks post-STZ, following the manufacturer's protocol.

Heart Digestion and Cell Separation

Whole hearts were harvested from killed animals and digested using digestion buffer, as previously described (21). After 30 min of digestion at 37°C, the cell suspension was filtered and plated onto tissue culture dishes for 2 h. This period allowed for the removal of the adherent fibroblast population. The nonadherent cells were incubated with sheep anti-rabbit IgG magnetic Dynabeads beads (Invitrogen) coated with CD31 antibody (Abcam) for 30 min at 4°C. The $CD31^+$ cells were pulled down using a magnet and constituted the EC fraction. The remainder of the cells from the $CD31^+$ cell sort was enriched for cardiomyocytes, with 80% of the cells confirmed to be cardiomyocytes by troponin staining and flow cytometry (data not shown).

GLO1 Activity

GLO1 activity was determined by measuring the rate of formation of *S*-D-lactoylglutathione from hemithioacetal, as previously described (20). Briefly, the assay mixture containing MG (7.9 mmol/L) was equilibrated to room temperature, and the reaction was initiated by the addition of lysate (10–50 mg). GLO1 activity is recorded as the mmol/L concentration of *S*-D-lactoylglutathione formed/min/mg of lysate protein (concentration determined by the bicinchoninic acid protein assay). GLO1 activity was measured in the whole heart, enriched cardiomyocyte cell population, and primary EC culture. Because number of ECs that could be obtained from myocardial tissue was insufficient for performing the GLO1 activity assay, ECs isolated from the aorta were used. GLO1 activity is presented as fold-change compared with the WT mice.

Western Blot

Protein expression analysis was determined by Western blots, as described previously (20). The levels of c-myc, tumor necrosis factor-α (TNF-α), receptor for AGE (RAGE), and neuregulin in the heart were assessed (antibodies from Abcam). For the detection of endothelial nitric oxide synthase (eNOS) dimers, polyacrylamide electrophoresis was performed using monomer/dimer-specific antibodies (Abcam) at low temperature (4°C), as previously described (22). Levels of angiopoietin 2 (antibody from Abcam) were assessed in lysates of human cardiac ECs (HCECs) after 24 h culture in different conditions (see LIVE/DEAD ASSAY). Densitometry data were analyzed using ImageJ software and normalized to tubulin expression.

Carbonyl Stress Measurements

Using an OxiSelect Protein Carbonyl ELISA kit, whole heart lysates were probed for total protein carbonyl content, according to the manufacturer's protocol. Briefly,

equal concentrations of protein lysates were loaded onto the plate and then transformed chemically to 2,4-dinitrophenyl (DNP) hydrazone and probed with an anti-DNP antibody, followed by a horseradish peroxidase–conjugated secondary antibody. The protein carbonyl content of the samples was determined by comparison against a standard curve of the predetermined reduced and oxidized BSA standards and expressed as nmol of carbonyl protein per mg of total protein.

Histology and Immunohistochemistry

Hearts were collected, perfused with saline, and then flash frozen in optimal cutting temperature compound for immunostaining of ECs by using von Willebrand factor (vWF), CD68, and CD31 antibodies (Abcam), and for cell death by using a TUNEL kit (Roche) or fixed in 4% formalin and embedded in paraffin in situ hybridization (ISH) (see ISH) and RAGE staining (Abcam). Visualization was performed, as described previously (20), using a Zeiss Axiophot microscope equipped with a Hamamatsu C5985 chilled CCD camera, and MetaMorph 4.01 imaging software (Molecular Devices). Cell counts were determined and averaged from five random fields of view (FOV).

ISH

ISH was performed, as previously described (23), using digoxigenin-labeled antisense RNA riboprobes prepared by in vitro transcription from linearized plasmids containing complete or partial cDNA sequences for hGlo1 and endothelin. Briefly, sections of heart tissue were hybridized overnight at 65°C in a humidified chamber, washed stringently, and incubated with an alkaline phosphatase-conjugated anti-digoxigenin antibody. Staining was performed using Nitro blue tetrazolium (Roche) and 5-bromo-4-chloro-3-indolyl phosphate (Roche) and analyzed on an Axioplan microscope. Digital images were captured using an AxioVision 2.05 camera (Zeiss).

Echocardiography

At 4 and 8 weeks post-STZ administration, LV ejection fraction (LVEF), fractional shortening (FS), and other heart-function measurements were determined by echocardiography on long-axis views with a Vevo 770 system (VisualSonics) in B mode with the use of a 707B series real-time microvisualization scanhead probe.

Macrophage Isolation and Culture

As previously described (24), bone marrow–derived (BMD) macrophages (BMDMs) were generated from tibia bone marrow of WT and GLO1 male mice (8–10 weeks old). BMDMs were maintained for 1 week in DMEM with 10% FBS, 15% L929 media containing macrophage colony-stimulating factor and penicillin-streptomycin. After 72 h of additional culture with or without 5 μmol/L MG, the release of TNF-α by BMDMs was assessed in culture supernatants by ELISA (eBioscience). Values were normalized to TNF-α content in the BMDM groups without MG treatment.

EC Culture

Cryopreserved Clonetics HCECs (Lonza) were grown in endothelial growth medium with the 2MV BulletKit media. All experiments were performed using cells at passage 2–4 in standard incubator conditions at 37°C and 5% CO_2 under normoxic conditions.

Cell Transfection

HCECs were seeded in 12-well plates (0.5 million cells/plate) using standard culture medium. After 24 h, the media was changed to Opti-MEM medium (Thermo Fisher), and cells were transfected with 20 μg plasmid DNA-lipofectin complex using the mammalian transfection kit (Thermo Fisher). The pCMV6-AC-GFP mammalian vector with COOH-terminal tGFP tag and hGLO1 cloning vector were obtained from OriGene. Transfection media was changed after 4 h, and cells were left to recover for 24 h. Transfection efficiency was 43% as determined by the GFP^+-to-GFP^- cell ratio, and a ninefold increase in hGLO1 expression was confirmed by PCR.

Live/Dead Assay

After 24 h of exposure to 30 mmol/L HG or 5 μmol/L MG, with or without 10 ng/mL TNF-α in the media, cells were washed with PBS and stained with propidium iodide (PI) (Invitrogen) for 30 min, according to the manufacturer's protocol, and imaged using a Zeiss Axiophot microscope. Cells whose nuclei were stained with PI (red) were considered dead, and those labeled green were considered positive for GLO1 transfection. For quantification, the total number of cells and the number of dead GFP^+ and dead GFP^- cells were counted in four random FOV per well.

Carbonyl Stress Measurements of HCECs

HCECs (50,000/well) were lysed after 24 h exposure to 30 mmol/L HG or 5 μmol/L MG with or without 10 ng/mL TNF-α. Protein carbonyl content was determined using the OxySelect ELISA kit according to the manufacturer's protocol.

RNA Extraction, cDNA Synthesis, and Quantitative PCR

Total RNA was extracted from $CD31^+$ cells separated from mouse hearts and blood mononuclear cells (GLO1 and WT mice) using Trizol reagent (Invitrogen), following the manufacturer's instructions. First-strand cDNA was synthesized from RNA (2 mg) using GoScript reverse transcriptase (Promega) and random hexamer primers (IDT). Levels of *Bcl-2* mRNA in $CD31^+$ cells and *hGLO1* in mononuclear cells were assessed by real-time quantitative PCR (qPCR) using LightCycler 480 SYBR Green I Master (Roche) and a LightCycler 480 Real-Time PCR system (Roche). Relative changes in mRNA expression of target genes were determined using the ΔΔCt method and expressed as levels relative to the combined average values of *18S* and *Gapdh*.

Statistical Analysis

Results are expressed as means ± SEM. Statistical analyses were performed using SigmaStat software. Comparisons

between two groups were made by an unpaired two-tailed Student *t* test. For multiple group comparisons, a one-way ANOVA with a post hoc Student-Newman-Keuls test was performed. Statistical significance was given for $P < 0.05$.

RESULTS

Increased GLO1 Expression and Activity in the Hearts of GLO1 Mice

It was confirmed that hGlo1 is not overexpressed in the cardiomyocytes of our transgenic mice. ISH demonstrated that the vasculature in the myocardial sections of GLO1 mice stained positive for hGlo1, whereas hGlo1 staining was not observed in the WT mice. The expression pattern of hGlo1 was similar to that of endothelin and vWF (Fig. 1*A*). When GLO1 activity was examined, the whole heart of transgenic mice exhibited a 1.8-fold increase in activity compared with the WT hearts (Fig. 1*B*). After heart digestion and cell isolation, no difference in GLO1 activity was detected in cardiomyocytes between GLO1 and WT mice, but aortic ECs extracted from GLO1 mice showed a 5.5-fold increase in GLO1 activity compared with the WT group (Fig. 1*B*). The presence of hGLO1 in aorta ECs was also confirmed by Western blot for the c-myc tag, which was not detected in the cardiomyocyte population (Fig. 1*C*). Expression of the hGlo1 gene was also found in the blood mononuclear cell fraction (mainly monocytes) of GLO1 mice but not in their WT littermates (data not shown).

Hyperglycemia-Induced Endothelial Inflammation Is Reduced by GLO1 Overexpression

After 8 weeks of hyperglycemia, WT-diabetic mice had increased circulating levels of the EC inflammation markers E-selectin, VCAM-1, and ICAM-1 compared with WT nondiabetic mice by 1.5-, 1.2-, and 1.4-fold, respectively ($P \leq 0.04$) (Table 1). GLO1 overexpression in the vasculature restored circulating levels of E-selectin, VCAM-1, and ICAM-1 to that of the nondiabetic mice ($P = 0.2$–0.7). Compared with the WT-diabetic mice, there was a significant reduction in the level of VCAM-1 ($P < 0.001$) and a trend for reduced E-selectin and ICAM-1 (both $P = 0.1$) in the serum of GLO1-diabetic mice (Table 1).

Inflammation Is Reduced in the Heart of Diabetic GLO1 Mice

To further explore the consequence of hyperglycemia in the heart, carbonyl stress was evaluated. ROS accumulation (not related only to MG accumulation) leads to protein oxidation and the formation of carbonyl groups on proteins, which can be measured by protein carbonyl assays. Carbonyl stress was increased in the whole heart of the WT-diabetic (by 2.5-fold) and GLO1-diabetic (1.8-fold) groups ($P \leq 0.008$) compared with the nondiabetic mice (Fig. 2*A*). There was a trend for less carbonyl stress in the GLO1-diabetic versus WT-diabetic mice by 20% ($P = 0.1$). Immunohistochemistry staining of tissue sections showed increased RAGE expression throughout the tissue in the WT-diabetic heart compared with the other groups (Fig. 2*B*). The myocardial protein content of RAGE was also increased only in the hearts from WT-diabetic mice versus all other groups by ≥1.8-fold ($P \leq 0.02$) (Fig. 2*C*). Both diabetic groups had greater expression of the inflammatory cytokine TNF-α (3.5-fold for WT-diabetic and 2-fold for GLO1-diabetic) compared with nondiabetic controls ($P \leq 0.02$) (Fig. 2*D*), but the GLO1-diabetic mice exhibited lower TNF-α versus the WT-diabetic group ($P = 0.04$). No difference was observed in the number of $CD68^+$ macrophages in the hearts of GLO1-diabetic versus WT-diabetic mice, but there was a trend for increased accumulation of macrophages in the diabetic mice by approximately twofold compared with nondiabetic controls ($P \leq 0.1$) (Fig. 2*E*).

TNF-α Secretion Reduced in Macrophages From GLO1 Mice

In vitro studies were performed to help explain the observation that TNF-α levels were reduced in the hearts of GLO1-diabetic mice despite having similar numbers of recruited macrophages compared with the WT-diabetic group. BMDMs from WT and GLO1 mice were cultured with or without 5 μmol/L MG, and the TNF-α content was measured in the supernatants by ELISA. BMDMs from WT mice had increased TNF-α secretion when exposed to MG compared with all other groups ($P \leq 0.03$) (Fig. 2*F*), whereas TNF-α secretion from BMDMs of GLO1 mice did not differ from BMDMs without MG exposure (Fig. 2*F*).

Increased GLO1 Activity Preserves EC Numbers and Prevents Cell Death in the Diabetic Mouse Heart

The number of ECs in the myocardium was assessed in tissue sections by vWF and CD31 staining. At 8 weeks post-STZ treatment, the number of vWF^+ ECs per FOV was reduced in WT-diabetic hearts (by 40%) compared with the other groups ($P \leq 0.001$) (Fig. 3*A* and *B*). Similar results were obtained with $CD31^+$ staining (data not shown; $P \leq 0.02$). Notably, despite the presence of hyperglycemia, GLO1-diabetic mice had no loss of ECs compared with the nondiabetic animals. $CD31^+$ ECs were sorted from harvested heart myocardium, and the mRNA level of the antiapoptotic gene *Bcl-2* was determined. *Bcl-2* expression was downregulated in WT-diabetic ECs compared with all other groups, whereas levels were not significantly different in $CD31^+$ cells from GLO1-diabetic mice compared with the nondiabetic controls (Fig. 3*C*). Apoptotic cells, determined by TUNEL staining, were more numerous in the hearts of WT-diabetic mice as early as 4 weeks post-STZ injection (up to 8.6-fold greater compared with all other groups, $P \leq 0.02$) (Fig. 3*D*). By 8 weeks post-STZ, the number of $TUNEL^+$ cells in WT-diabetic mice increased to 10-fold greater than controls ($P \leq 0.006$). For GLO1-diabetic mice, there was no difference in the number of apoptotic cells at 4 weeks compared with the nondiabetic mice. However, at 8 weeks, GLO1-diabetic mice had a 4.1-fold increase in $TUNEL^+$ cells compared with control mice ($P = 0.045$), but this was still fewer (2.5-fold less) than in WT-diabetic mice ($P = 0.008$) (Fig. 3*D*).

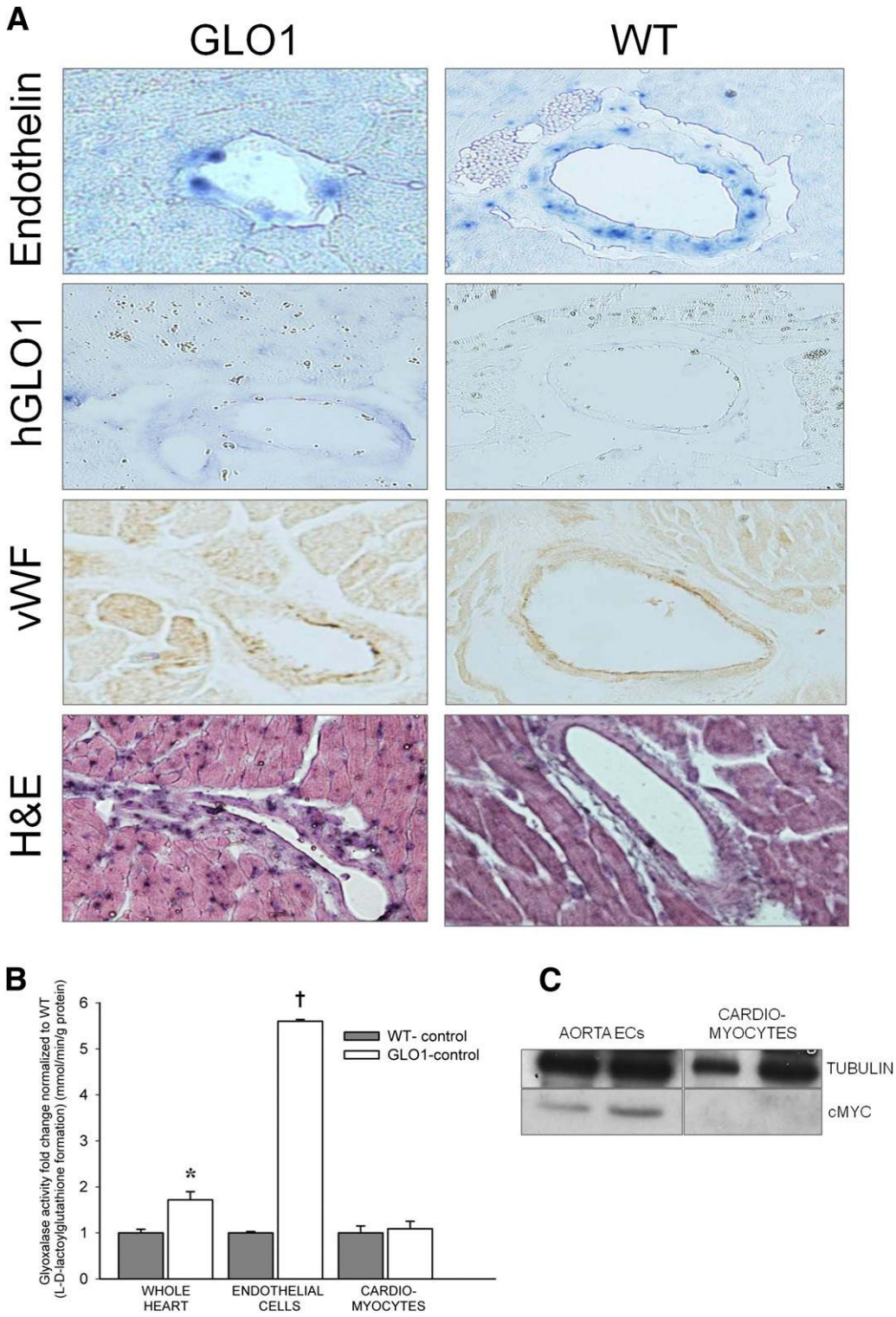

Figure 1—Overexpression of hGlo1 was confirmed in the ECs of GLO1 mouse hearts. *A*: In situ staining of proendothelin and hGlo1 showed mRNA expression of endothelin in WT and GLO1 mice, whereas hGlo1 mRNA was present only in GLO1 transgenic mice. Staining of ECs/vasculature was confirmed by vWF and hematoxylin and eosin (H&E) staining. *B*: GLO1 activity measured in the whole heart, ECs, and cardiomyocytes ($n = 5$). *$P = 0.01$ vs. whole heart WT-control; †$P < 0.01$ vs. endothelial cells WT-control. *C*: Representative cMYC Western blots of aortic ECs and cardiomyocytes from GLO1 mice show the presence of the tagged GLO1 protein only in ECs (each lane represents a different mouse).

Table 1—Concentration of soluble endothelial adhesion molecules in blood serum

	WT-control	GLO1-control	WT-diabetic	GLO1-diabetic
E-selectin (pg/mL)	758.9 ± 22.6	956.1 ± 156.0	1,149.4 ± 51.5*	825.7 ± 172.4
VCAM-1 (pg/mL)	39.0 ± 0.7	39.1 ± 0.7	45.0 ± 0.6†	39.8 ± 1.3
ICAM-1 (pg/mL)	14.3 ± 0.3	15.4 ± 1.1	19.9 ± 1.7‡	17.4 ± 0.1

ELISA measurement of EC inflammation markers in blood serum of mice at 8 weeks post-STZ (n = 3). *P = 0.002 vs. WT-control. †$P < 0.001$ vs. all other groups. ‡$P \leq 0.04$ vs. WT-control and GLO1-control.

Production of EC Proteins Is Preserved in GLO1-Diabetic Mice

EC proteins important for the support of a healthy myocardium (eNOS and neuregulin) were maintained in GLO1-diabetic mice. Specifically, the protein levels of eNOS, implicated in the regulation of vascular function and promotion of cardiomyocyte survival (25), were preserved in GLO1-diabetic mice (Fig. 4*A*). Current research suggests that only the dimeric form of eNOS is able to generate NO, whereas the ROS-induced monomeric form of eNOS produces superoxide instead (22). Although eNOS dimerization was reduced by 50% in WT-diabetic mice ($P \leq 0.04$), GLO1-diabetic mice maintained a level of dimeric eNOS similar to nondiabetic mice (P = 0.63) (Fig. 4*A*). The growth factor neuregulin produced in ECs is important in promoting cardiomyocyte function and survival (26). In WT-diabetic mice, neuregulin levels were ~75% less than in nondiabetic mice ($P \leq 0.05$) (Fig. 4*B*), but neuregulin expression was not significantly different between the GLO1-diabetic mice and controls.

GLO1 Overexpression in the Vasculature Delays STZ-Induced LV Dysfunction

There was no difference in LV function between WT and transgenic mice at baseline. At 4 weeks post-STZ, WT-diabetic mice exhibited reduced FS compared with all other groups ($P \leq 0.045$) (Fig. 5*A*). At 8 weeks, decreased LVEF and FS were observed in WT-diabetic and GLO1-diabetic mice compared with the nondiabetic mice ($P \leq 0.03$); however, LVEF and FS were significantly greater in GLO1-diabetic versus WT-diabetic mice ($P \leq 0.01$) (Fig. 5*A* and *B*). At 8 weeks, an increase in the heart-to-body mass ratio was found in both diabetic groups (5 ± 0.09 mg/g in WT-diabetic and 5 ± 0.21 mg/g in GLO1-diabetic mice compared with 4.4 ± 0.1 mg/g in nondiabetic mice, $P \leq 0.02$). This was most probably associated with body mass differences between the groups (nondiabetic mice weighed 26 ± 0.4 g, and diabetic mice weighed 20 ± 0.5 g, $P < 0.001$). Furthermore, the heart weight was reduced in both diabetic groups (P = 0.04). At 4 weeks, WT-diabetic mice showed reduced stroke volume, reduced cardiac output, and lowered diastolic end pressure compared with all other groups ($P \leq 0.02$) (Table 2), showing the first signs of heart failure. There was no difference in LV wall thickness or systolic end volume among the groups, but cardiac output, stroke volume, and diastolic end volume were all decreased at 8 weeks in both diabetic groups compared with control animals ($P \leq 0.03$) (Table 2). Still, between the two diabetic groups, cardiac output and stroke volume were significantly better in the GLO1 mice ($P \leq 0.04$) (Table 2), confirming the partial preservation of heart function by protection of the vasculature from MG.

HG or MG and TNF-α Synergize to Induce EC Death

From our in vivo observations, we hypothesized that HG/MG increases the sensitivity of ECs to TNF-α death signals. To elucidate possible mechanisms, carbonyl stress was first assessed by ELISA in cultures of human ECs. Protein carbonyls were increased in ECs treated with HG or MG for 24 h, regardless of the presence or absence of TNF-α ($P \leq 0.04$) (Fig. 6*A*). The expression of Ang-2 and *Bcl-2*, potentially involved in the combined effect of HG or MG with or without TNF-α on cell death, was then examined. ECs exposed to HG or MG with or without TNF-α had increased expression of Ang-2 protein compared with their respective control cultures ($P \leq 0.05$) (Fig. 6*B*). Notably, the combination of MG and TNF-α increased Ang-2 expression in ECs by 3.3-fold compared with cells exposed to MG without TNF-α (P = 0.049) (Fig. 6*B*). The exposure of ECs to MG or HG conditions also reduced mRNA expression of the antiapoptotic gene *Bcl-2*, regardless of the presence or absence of TNF-α ($P \leq 0.04$) (Fig. 6*C*). Finally, the combined effect of HG or MG with or without TNF-α on EC death was evaluated. The percentage of apoptotic cells (PI^+) was increased for ECs treated for 24 h with HG or MG in the presence of TNF-α ($P \leq 0.04$) (Fig. 6*D*). Notably, ECs transfected with GLO1/GFP were protected when cultured under these same conditions, with significantly less cell death observed in MG, HG+TNF-α, and MG+TNF-α conditions compared with their respective nontransfected controls ($P \leq 0.02$) (Fig. 6*D*).

DISCUSSION

The aim of this study was to elucidate a link between MG, EC inflammation, and reduced cardiac function. To this end, we used a transgenic mouse model in which the vasculature is protected from MG by GLO1 overexpression. We demonstrated that GLO1 overexpression in the vasculature of hyperglycemic (type I diabetic) mice: *1*) reduced vascular inflammation; *2*) preserved cardiac EC viability and protein production (*Bcl-2*, eNOS, and neuregulin); *3*) reduced overall cell death in the myocardium; and *4*) delayed and limited the loss of cardiac function. These

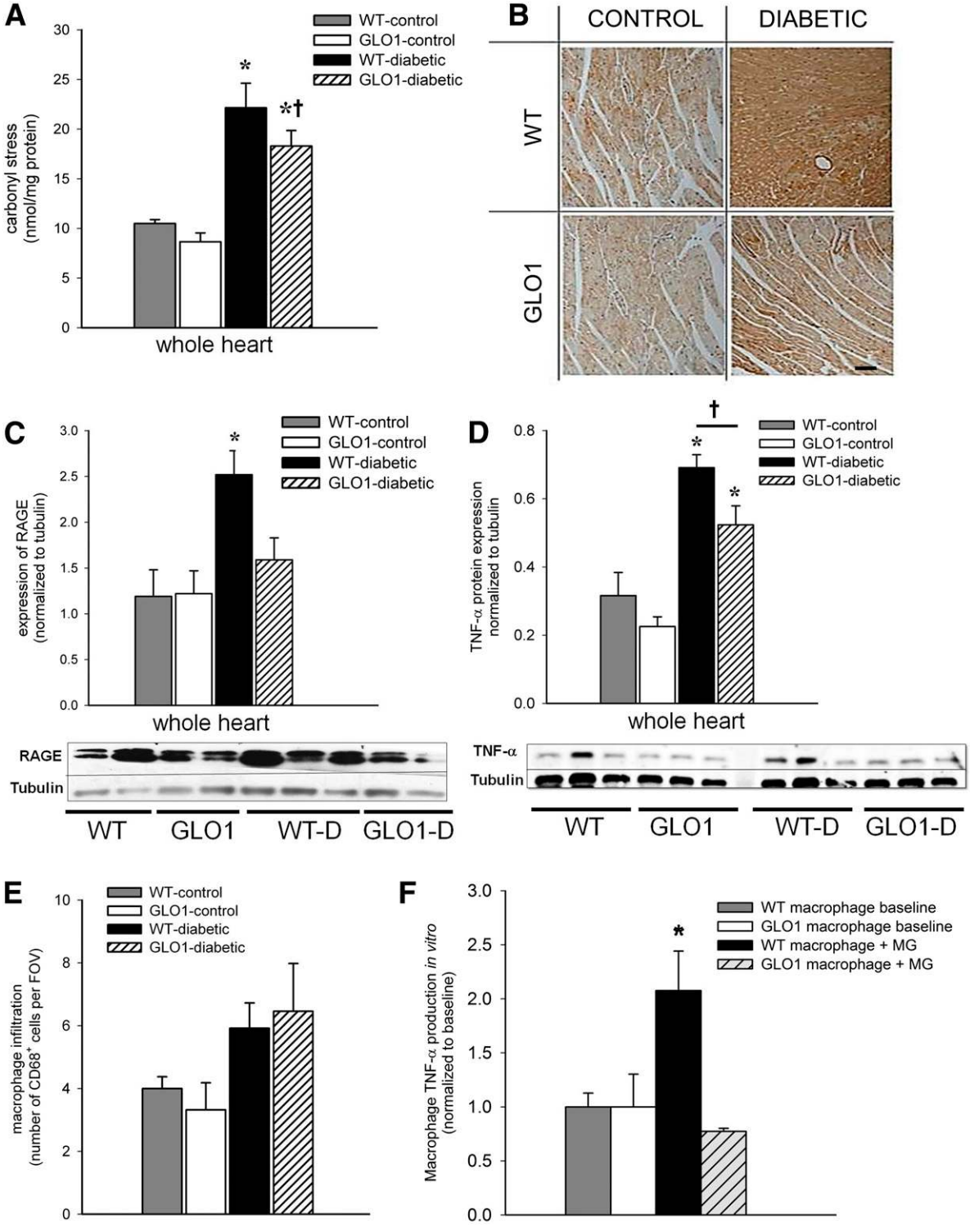

Figure 2—GLO1 overexpression reduces inflammation in the myocardium of diabetic mice. *A*: ELISA analysis of protein carbonization in the myocardium at 8 weeks as a measure of oxidative stress (n = 3–4 per group). *$P \leq 0.008$ vs. WT- and GLO1-control mice; †$P = 0.1$ vs. WT-diabetic mice. *B*: Representative images of RAGE staining in the myocardium at 8 weeks. Scale bar = 50 μm. *C*: Representative Western blot and quantification of RAGE protein in myocardial tissue at 8 weeks (n = 4–5). *$P \leq 0.02$ vs. all other groups. *D*: Representative Western blot and quantification of TNF-α in myocardial tissue at 8 weeks (n = 3). *$P \leq 0.02$ vs. WT- and GLO1-control mice; †$P = 0.04$. *E*: Quantification of macrophages ($CD68^+$ cells) in sections of myocardial tissue at 8 weeks (number/FOV; n = 4–5). *F*: Secretion of TNF-α by BMDMs isolated from WT and GLO1 mice after 72 h of culture with or without MG (n = 4). *$P \leq 0.03$ vs. all other groups.

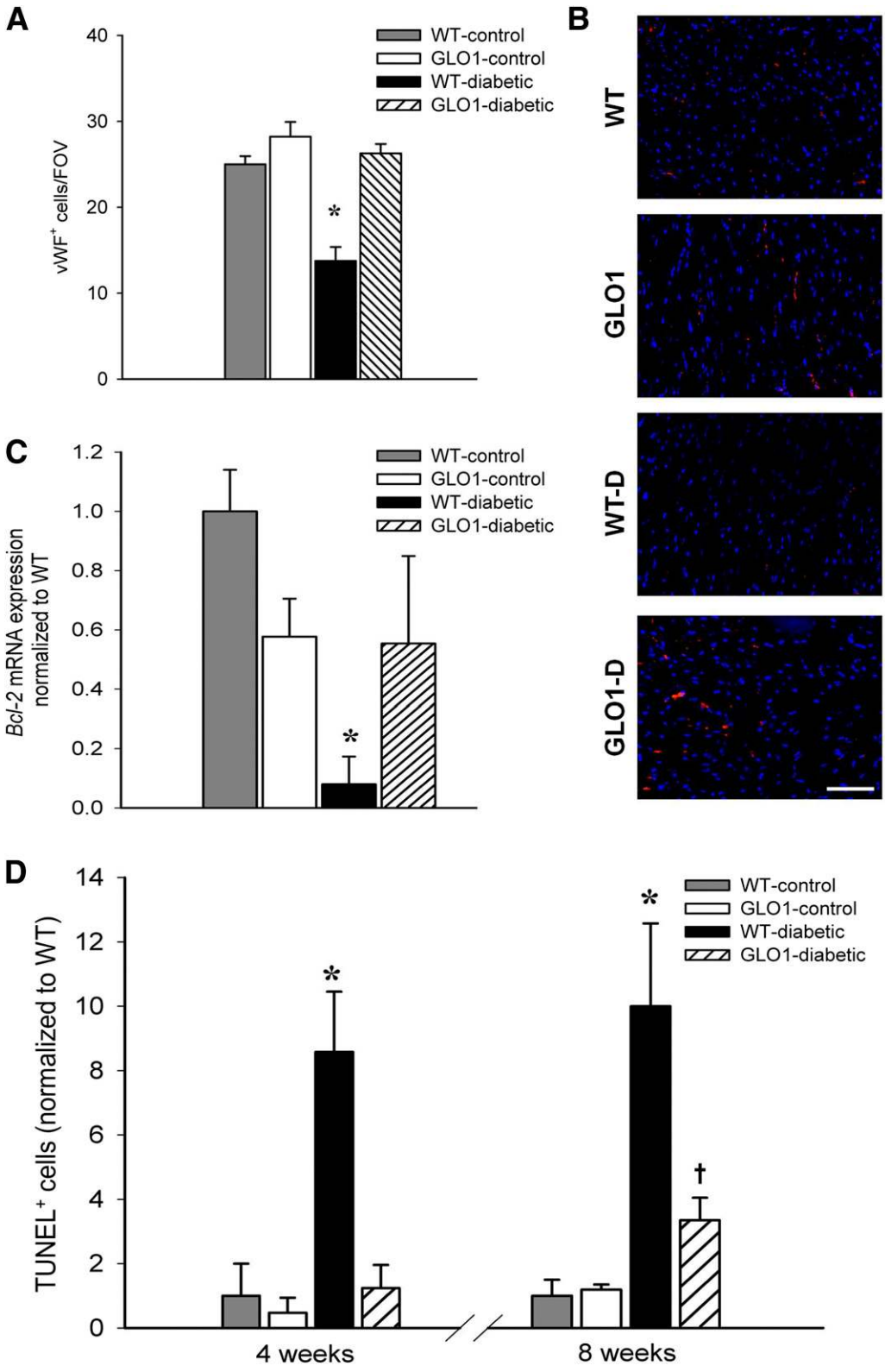

Figure 3—GLO1 overexpression promotes EC survival in the myocardium of diabetic mice. *A*: Number of vWF$^+$ ECs per FOV in myocardial tissue sections at 8 weeks (n = 3–4 per group). *$P \leq 0.001$ vs. all other groups. *B*: Representative images of vWF staining (red) with DAPI-stained cell nuclei (blue). Scale bar = 10 μm. *C*: Expression of the antiapoptotic gene *Bcl-2* in CD31$^+$ ECs isolated from the myocardium at 8 weeks (n = 3). *$P \leq 0.03$ vs. all other groups. *D*: The percentage of TUNEL$^+$ apoptotic cells per FOV normalized to the percentage observed in WT mice at 4 and 8 weeks (n = 3–4 per group). *$P \leq 0.02$ vs. all other groups at 4 weeks; *$P \leq 0.008$ vs. all other groups at 8 weeks; †$P = 0.045$ vs. WT- and GLO1-control mice.

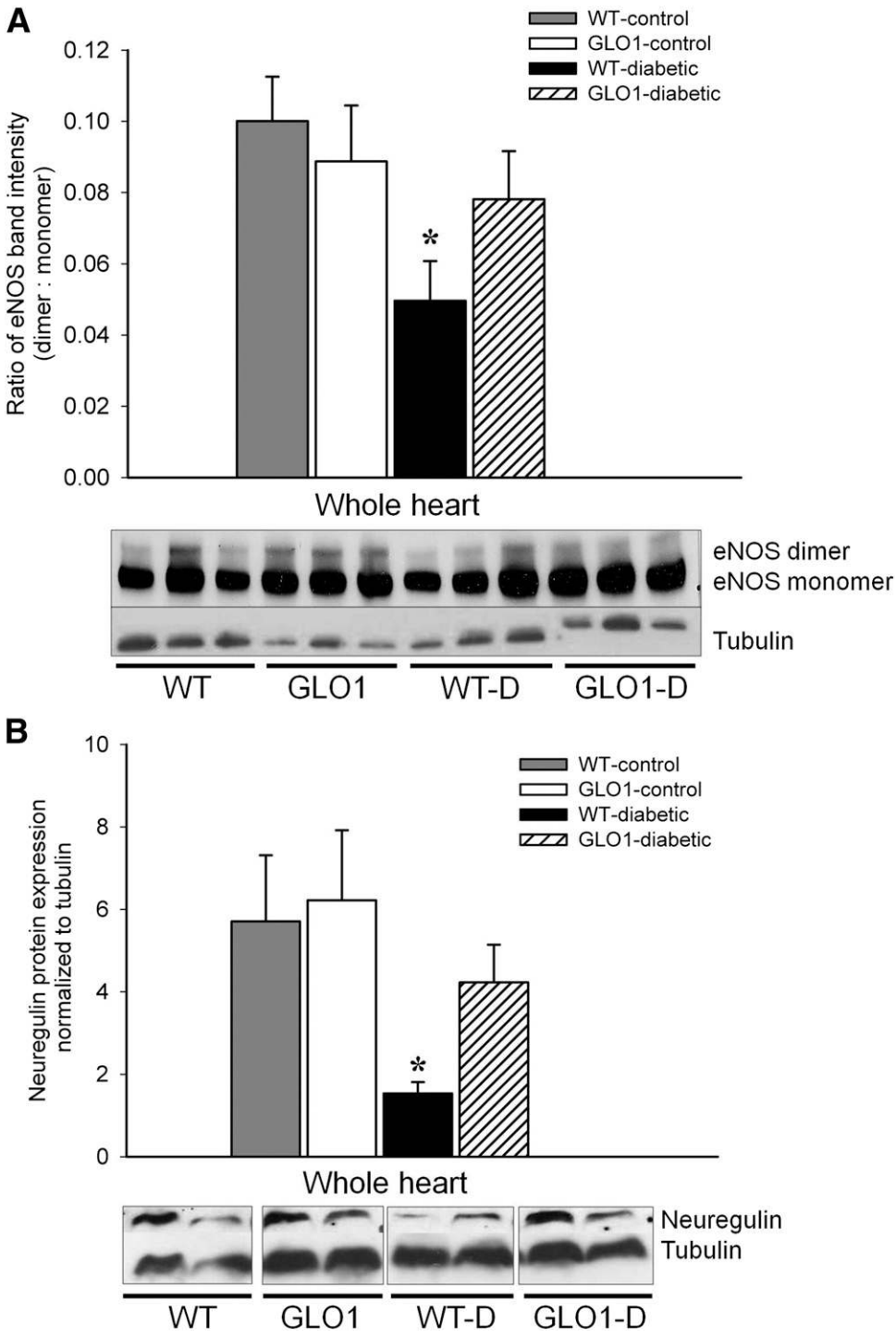

Figure 4—The production of eNOS and neuregulin is maintained in the hearts of GLO1-diabetic mice. *A*: Representative Western blot and quantification of the eNOS dimer-to-monomer ratio in the myocardium at 8 weeks (n = 3). *$P \leq 0.04$ vs. WT- and GLO1-control mice. *B*: Representative Western blot and quantification of neuregulin protein in the myocardium at 8 weeks (n = 4). *$P \leq 0.05$ vs. WT- and GLO1-control mice.

results highlight the importance of MG-induced endothelial inflammation in the development of ventricular dysfunction in diabetes.

To establish that our GLO1 mice provided a good model for this study, we confirmed that the localization of hGlo1 and the associated increase in GLO1 activity were both restricted to the ECs and the vasculature of the myocardium. Furthermore, Western blot analysis of whole heart tissue showed no difference in the levels of MG-H1 (the major product of MG-specific glycation) between

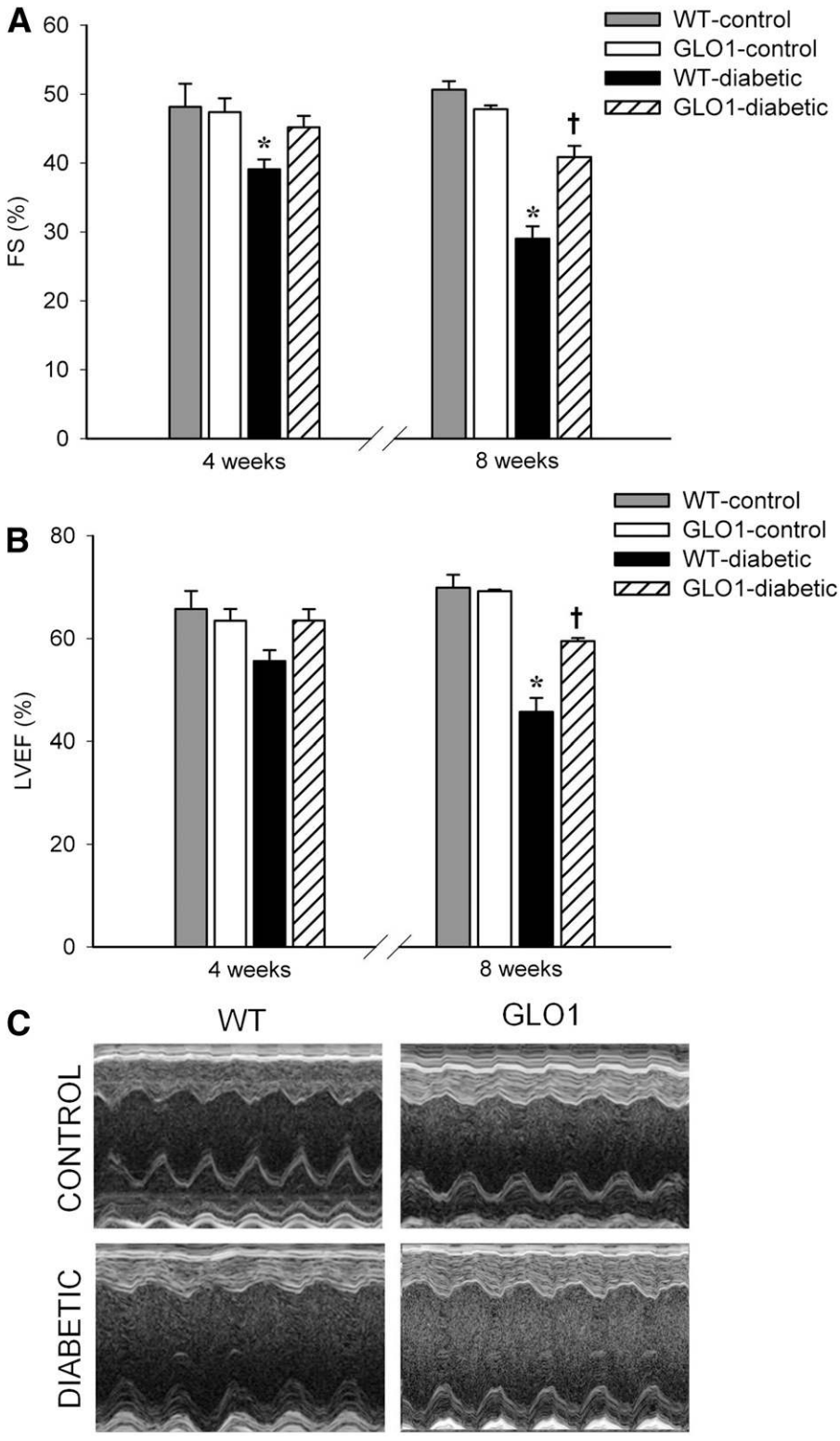

Figure 5—GLO1 overexpression delays and limits the loss of cardiac function in diabetic mice. *A*: FS measured by echocardiography at 4 and 8 weeks (n = 8 each time). *$P \leq 0.045$ vs. all other groups at 4 weeks; *$P < 0.001$ vs. all other groups at 8 weeks; †$P \leq 0.02$ vs. WT- and GLO1-control mice at 8 weeks. *B*: LVEF measured by echocardiography at 4 and 8 weeks (n = 8 each time). *$P \leq 0.01$ vs. all other groups at 8 weeks; †$P \leq 0.03$ vs. WT- and GLO1–control mice at 8 weeks. *C*: Representative echocardiogram recordings for nondiabetic and diabetic mice.

GLO1 and WT mice (data not shown). Thus, cardiomyocytes in GLO1 mice are expected to still be susceptible to the harmful effects of HG and MG accumulation, and changes in heart function after STZ was administered can be attributed to protection conferred by the ECs and vasculature. In addition, as discussed later in this section, reduced MG in monocytes and/or macrophages of GLO1 mice may also alleviate the effects of diabetes.

To assess the presence and severity of EC activation and inflammation, we measured the levels of the soluble adhesion molecules VCAM-1, ICAM-1, and E-selectin in blood serum. The release of VCAM-1, ICAM-1, and E-selectin into the circulation is an indicator of EC inflammation and/or cell death (27,28). Notably, GLO1 overexpression protected the ECs in diabetic mice, because increased VCAM-1, ICAM-1, and E-selectin levels were not present in the GLO1-diabetic mice as they were in the WT-diabetic group.

Myocardial inflammation is one of the main contributors to heart failure (29). In the current study, the increased carbonyl stress, RAGE expression, and inflammatory cytokine production (TNF-α) provided evidence of inflammation in the WT-diabetic mice. The overexpression of GLO1 reduced this inflammatory state but did not completely prevent it. The level of carbonyl stress is an indirect measure of oxidative stress through the detection of carbonylated proteins (30). Because the cardiomyocytes in GLO1 mice were not protected from MG, it is reasonable to expect that their level of carbonyl stress would be similar to that of WT-diabetic mice. Cardiomyocytes represent the largest contributor to myocardial mass, yet the hearts of GLO1 mice exhibited a trend for reduced levels of carbonylated proteins. Whether this result is exclusively from reduced carbonyl stress in the vasculature or also through an undetermined secondary protective effect conferred to cardiomyocytes by the ECs was not elucidated in the current study. Regardless, this highlights the importance of ECs and the vasculature in the overall regulation of inflammation and stress in the diabetic heart.

The loss of EC number and function in diabetes is well described (31) and largely occurs due to the accumulation of MG (32,33). In our study, the detrimental effect of hyperglycemia on ECs was evident: the number of vWF^+ and $CD31^+$ ECs was reduced in the hearts of WT-diabetic mice, and neuregulin and eNOS expression was reduced. However, the number of vWF^+ and $CD31^+$ ECs was preserved in the GLO1-diabetic mice compared with the nondiabetic groups, suggesting that increased MG caused EC loss in the heart. The improved survival of ECs in GLO1-diabetic mice may be related to the preserved mRNA levels of the antiapoptotic gene *Bcl-2*, which have been shown to be modified by MG (34). In addition to improved EC survival, the levels of neuregulin and eNOS in cardiac ECs were maintained in GLO1-diabetic but not in WT-diabetic mice compared with the nondiabetic controls.

Table 2—The effect of diabetes and GLO1 overexpression on cardiac function

	WT-control		GLO1-control		WT-diabetic		GLO1-diabetic	
	4 weeks	8 weeks	4 weeks	8 weeks	4 weeks	8 weeks	4 weeks	8 weeks
Wall thickness (mm)	0.87 ± 0.01	0.88 ± 0.01	0.87 ± 0.01	0.87 ± 0.01	0.83 ± 0.01	0.83 ± 0.01	0.85 ± 0.01	0.85 ± 0.01
Cardiac output (mL)	13.6 ± 0.7	12.2 ± 1.4	12.5 ± 0.7	11.2 ± 0.7	9.6 ± 0.2*	6.8 ± 0.5†	10.9 ± 0.2	8.4 ± 0.19‡§
Stroke volume (mL)	34.6 ± 1.9	33.6 ± 1.8	32.4 ± 0.9	30.4 ± 1.8	21.4 ± 0.9*	20.5 ± 0.9†	29.6 ± 0.4	24.8 ± 1.2‡§
End volume (mL)								
Diastole	50.1 ± 1.6	49.7 ± 2.3	50.7 ± 3.2	48.9 ± 2.8	37.9 ± 0.8*	38.4 ± 1.1†	46.0 ± 2.2	39.3 ± 2.4‡
Systole	16.5 ± 0.7	18.1 ± 2.7	15.9 ± 2.1	18.5 ± 1.8	16.5 ± 0.8	16.7 ± 1.7	17.8 ± 0.2	15.8 ± 1.0
Blood glucose level (mmol/L)	n/a	5.4 ± 0.2	n/a	5.8 ± 0.3	19.5 ± 1.9	20.7 ± 1.1†	14.9 ± 1.7	19.1 ± 1.3†

Echocardiography results for various cardiac function parameters assessed at 4 and 8 weeks post-STZ (n = 6–8 per group). n/a, not applicable. *$P \leq 0.02$ vs. all other groups at 4 weeks. †$P \leq 0.01$ vs. WT- and GLO1-control at 8 weeks. ‡$P \leq 0.03$ vs. WT- and GLO1-control at 8 weeks. §$P \leq 0.04$ vs. WT-diabetic at 8 weeks.

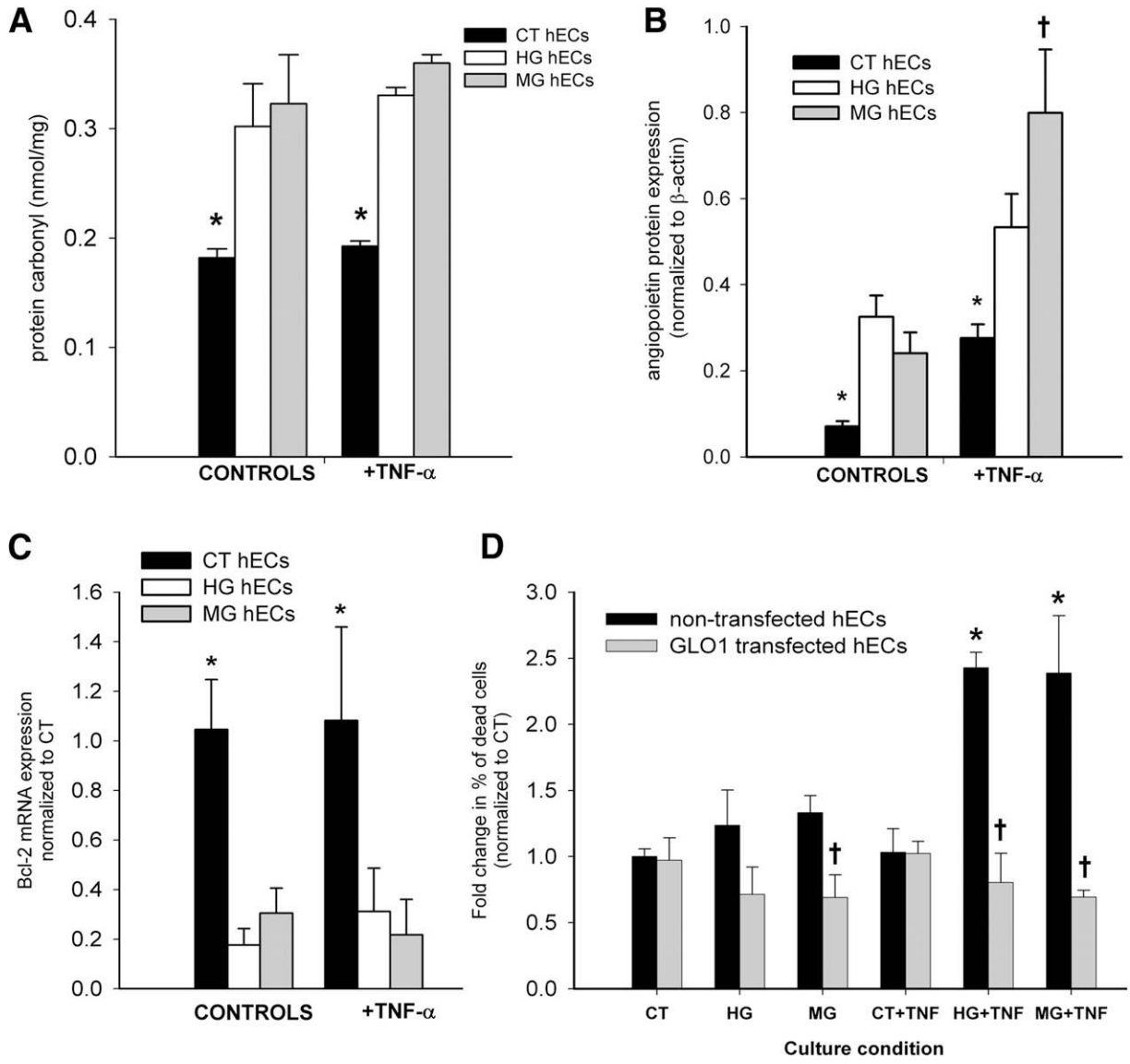

Figure 6—HG or MG in combination with TNF-α act synergistically to negatively affect human EC (hEC) properties and viability. *A*: Protein carbonyls (nmol/mg) formed in hECs after 24 h (n = 3). *$P \leq 0.04$ compared with HG or MG treatment with or without TNF-α. *B*: Quantification of Ang-2 protein expression in hECs exposed to HG or MG with or without TNF-α (n = 3). *$P \leq 0.05$ vs. other groups within condition; †$P = 0.049$ vs. MG-control group. *C*: Relative expression of *Bcl-2* mRNA is reduced in hECs 24 h after treatment with HG or MG (n = 3). *$P \leq 0.04$ compared with HG or MG with or without TNF-α treatment. *D*: The combined effect of HG (30 mmol/L) or MG (5 μmol/L) with or without TNF-α (10 ng/mL) on the death of GLO1/GFP transfected and control hECs was assessed after 24 h. The percentage of dead control and/or GLO1 transfected ECs was determined by PI staining (n = 3–4). *$P \leq 0.04$ vs. controls; †$P \leq 0.02$ vs. nontransfected cells in same condition). CT, control.

Neuregulin produced by ECs closely adjoined to cardiomyocytes in the adult heart helps to regulate cardiomyocyte contractility and survival under stress conditions (35). It has been shown that neuregulin is reduced in diabetes (36), but ours is the first study to show that protecting ECs from MG can prevent this effect. Diabetes also reduces the amount of dimeric eNOS (22). The lack of this form of eNOS reduces NO production, which negatively affects the regulation of vascular function and the response of cardiomyocytes to stress while increasing the deleterious production of superoxide. Changes in NO/redox-based signaling contribute to cardiovascular dysfunction and programmed cell death (25). Mechanisms by which MG affects eNOS status have been reported. For example, MG modifications of hypoxia-inducible factor 1α have been shown to reduce eNOS expression in BMD endothelial progenitor cells, which was prevented by GLO1 overexpression (37). GLO1 can reduce the inhibitory phosphorylation of eNOS caused by MG and neutralize vascular aging (38). In our study, the overexpression of GLO1 preserved the eNOS dimerization process. It should be noted that neuregulin and NO are just two components

involved in EC-cardiomyocyte signaling and that other factors not evaluated in the current study may contribute to the superior cardiac function observed in GLO1-diabetic mice. However, because GLO1 overexpression maintained EC number and production of eNOS and neuregulin, altered expression of these other potential contributing factors must also likely be a consequence of modified MG levels.

A similar observation was made for TNF-α expression: levels were elevated in the hearts of WT-diabetic mice and reduced by overexpressing GLO1. TNF-α is produced mainly in macrophages, and elevated levels of TNF-α in patients with diabetes are associated with micro- and macrovascular complications (39). MG has been shown to stimulate the production and secretion of TNF-α from macrophages (40), which was also observed in our in vitro BMDMs studies. The GLO1- and WT-diabetic groups had a trend for increased numbers of macrophages in the heart compared with nondiabetic mice; but notably, the blood mononuclear cells (this study) and macrophages of GLO1 mice (18) have been shown to have increased GLO1 expression. Therefore, GLO1 overexpression in macrophages may be contributing to reduced inflammation and cell death in GLO1 mice in the current study. This could potentially make them less susceptible to MG-induced TNF-α production and provides a plausible explanation for the reduced TNF-α level in the hearts of GLO1-diabetic mice. This scenario is supported by in vitro data showing that macrophages from GLO1 mice did not increase TNF-α secretion when exposed to MG, unlike the macrophages from WT mice. Consequently, because TNF-α induces EC dysfunction and apoptosis (41), less TNF-α secreted by macrophages may contribute to the improved health of the ECs and vasculature observed in GLO1 mice. Although reduced compared with WT-diabetic mice, TNF-α levels in GLO1-diabetic mice were still greater than in nondiabetic mice. This suggests that TNF-α may be originating from another source, such as cardiomyocytes, which has been previously reported (42).

In vitro studies were performed to further elucidate a mechanism for MG-induced EC inflammation and death. The results showed that MG increased carbonyl stress and Ang-2 protein, reduced *Bcl-2* expression in HCECs, and acted synergistically with TNF-α to induce death. HG has been shown to increase the expression of Ang-2, ICAM, and VCAM in ECs, and HG-induced Ang-2 expression sensitizes ECs to the proinflammatory effects of TNF-α (43,44). Similarly, in this study, Ang-2 protein expression increased in ECs exposed to HG or MG, and levels increased further in cells with combined MG+TNF-α treatment. These results provide mechanistic insight into the observation that WT-diabetic mice had increased TNF-α levels and EC death, whereas GLO1-diabetic mice did not have a similar loss of ECs. The lower TNF-α levels in GLO1-diabetic mice, along with possible reduced Ang-2 in ECs, may be contributing to reduce endothelial inflammation and preventing cell death. Notably, transfecting ECs with GLO1 completely protected them from death when cultured in combined HG or MG+TNF-α conditions, whereas a significant increase in cell death was seen for the nontransfected cells, thus supporting the in vivo observations.

Increased RAGE and RAGE ligand expression can further propagate inflammation and result in long-term complications of diabetes (45). RAGE is expressed in cardiomyocytes, vascular cells, fibroblasts, and infiltrating inflammatory cells in diabetes (46). Ligand binding of RAGE initiates a positive feedback loop whereby the receptor-ligand interaction triggers increased RAGE expression (47). Previous studies have shown that increased GLO1 activity reduces the accumulation of MG-derived AGEs (18,48). Furthermore, the production of endogenous RAGE ligands, such as S100 calgranulins and high mobility group box 1, is increased by hyperglycemia, which can be prevented by GLO1 overexpression (49). In our study, the expression of RAGE protein in GLO1-diabetic mice was reduced compared with the WT-diabetic group, despite similar levels of hyperglycemia. This may be associated with lower levels of RAGE ligands (e.g., MG-derived AGEs, high mobility group box 1, S100 calgranulins) in the GLO1 mice, thus reducing the positive-feedback upregulation of RAGE expression. Such a mechanism may be contributing to the observed decrease in inflammation in the GLO1-diabetic mice.

Protecting the vascular system from the effects of MG through GLO1 overexpression resulted in reduced overall cell death in the mouse heart. Although apoptosis was increased in WT-diabetic mice at 4 and 8 weeks post-STZ injection, GLO1-diabetic mice exhibited an increase in apoptotic $TUNEL^+$ cells only at 8 weeks but were still fewer than in the WT-diabetic group. Cardiomyocyte loss is an important mechanism in the process of myocardial remodeling, cardiac fibrosis, reduced heart function, and ultimately, heart failure (50). A previous study showed that ubiquitous overexpression of GLO1 in rats could attenuate cardiac fibrosis that otherwise developed in WT-diabetic rats after 16 weeks (48). We did not detect significant fibrosis in our WT-diabetic mice (1.3-fold, P = 0.1; data not shown), possibly because 8 weeks may be premature for full fibrosis development. Nevertheless, we observed reduced LV function in WT-diabetic mice as early as 4 weeks post-STZ, which was prevented in GLO1-diabetic mice.

Consistent with previous studies (2,48), the data presented here demonstrate the damaging effect of diabetes on cardiac function in mice. Evaluation of our mice at 4 and 8 weeks post-STZ allowed us to detect differences in the early stages of reduced cardiac function. LVEF and FS were already reduced after 4 weeks of hyperglycemia, which worsened along with other measures of cardiac function (cardiac output, systolic and diastolic end volume, heart weight) by 8 weeks compared with nondiabetic mice. Heart function of the GLO1-diabetic mice was superior to that of the WT-diabetic group, with a delay in

the onset of functional loss (observed only at 8 weeks), which was also of lesser magnitude. Although the chosen mouse model allowed us to isolate the effects of hyperglycemia and MG on heart function in a relatively short period, a limitation is that hyperglycemia was maintained throughout the study protocol, which is not necessarily representative of patients with diabetes who develop heart failure after longer periods of fluctuating glucose levels.

In summary, our findings suggest that preventing EC inflammation can improve myocardial function in the setting of hyperglycemia and MG accumulation. The complete mechanism(s) responsible for reduced inflammation and the protection against EC loss is complex, but our study identified some pathways that may be involved (e.g., GLO1 overexpression reduces TNF-α–mediated effects). Therefore, protecting the vasculature from MG may be a target for future studies and therapy to postpone and reduce the development of heart failure in diabetes.

Acknowledgment. The authors thank Rick Seymour (University of Ottawa Heart Institute) for technical support.

Funding. This work was supported by operating grants from the Heart & Stroke Foundation of Canada (000225 to R.W.M. and E.J.S.), the Canadian Institutes of Health Research (FRN 125678 to E.J.S.), and the National Institutes of Health (DK-020541 to F.G. and M.B.). B.V. was supported by a Canadian Graduate Scholarship from the Canadian Institutes of Health Research and B.M. by a research fellowship from the Heart & Stroke Foundation of Canada.

Duality of Interest. No potential conflicts of interest relevant to this article were reported.

Author Contributions. M.B., R.W.M., and E.J.S. designed the research. B.V., B.M., F.G., K.M., and N.J.R.B. performed the research. B.V., B.M., M.B., R.W.M., and E.J.S. analyzed data and wrote the manuscript. E.J.S. is the guarantor of this work and, as such, had full access to all data in the study and takes responsibility for the integrity of the data and the accuracy of the data analysis.

References

1. Hayat SA, Patel B, Khattar RS, Malik RA. Diabetic cardiomyopathy: mechanisms, diagnosis and treatment. Clin Sci (Lond) 2004;107:539–557

2. Poornima IG, Parikh P, Shannon RP. Diabetic cardiomyopathy: the search for a unifying hypothesis. Circ Res 2006;98:596–605

3. Boudina S, Abel ED. Diabetic cardiomyopathy, causes and effects. Rev Endocr Metab Disord 2010;11:31–39

4. Xu J, Zou MH. Molecular insights and therapeutic targets for diabetic endothelial dysfunction. Circulation 2009;120:1266–1286

5. Hadi HA, Suwaidi JA. Endothelial dysfunction in diabetes mellitus. Vasc Health Risk Manag 2007;3:853–876

6. Giacco F, Brownlee M. Oxidative stress and diabetic complications. Circ Res 2010;107:1058–1070

7. Thornalley PJ. Glyoxalase I–structure, function and a critical role in the enzymatic defence against glycation. Biochem Soc Trans 2003;31:1343–1348

8. Abordo EA, Minhas HS, Thornalley PJ. Accumulation of α-oxoaldehydes during oxidative stress: a role in cytotoxicity. Biochem Pharmacol 1999;58:641–648

9. Lapolla A, Flamini R, Dalla Vedova A, et al. Glyoxal and methylglyoxal levels in diabetic patients: quantitative determination by a new GC/MS method. Clin Chem Lab Med 2003;41:1166–1173

10. Brouwers O, Niessen PM, Haenen G, et al. Hyperglycaemia-induced impairment of endothelium-dependent vasorelaxation in rat mesenteric arteries is mediated by intracellular methylglyoxal levels in a pathway dependent on oxidative stress. Diabetologia 2010;53:989–1000

11. Turkseven S, Ertuna E, Yetik-Anacak G, Yasa M. Methylglyoxal causes endothelial dysfunction: the role of endothelial nitric oxide synthase and AMP-activated protein kinase α. J Basic Clin Physiol Pharmacol 2014;25:109–115

12. Brown A, Reynolds LR, Bruemmer D. Intensive glycemic control and cardiovascular disease: an update. Nat Rev Cardiol 2010;7:369–375

13. Dhar A, Dhar I, Desai KM, Wu L. Methylglyoxal scavengers attenuate endothelial dysfunction induced by methylglyoxal and high concentrations of glucose. Br J Pharmacol 2010;161:1843–1856

14. Sena CM, Matafome P, Crisóstomo J, et al. Methylglyoxal promotes oxidative stress and endothelial dysfunction. Pharmacol Res 2012;65:497–506

15. Lemmens K, Doggen K, De Keulenaer GW. Role of neuregulin-1/ErbB signaling in cardiovascular physiology and disease: implications for therapy of heart failure. Circulation 2007;116:954–960

16. Tirziu D, Giordano FJ, Simons M. Cell communications in the heart. Circulation 2010;122:928–937

17. Rössig L, Haendeler J, Mallat Z, et al. Congestive heart failure induces endothelial cell apoptosis: protective role of carvedilol. J Am Coll Cardiol 2000;36:2081–2089

18. Geoffrion M, Du X, Irshad Z, et al. Differential effects of glyoxalase 1 overexpression on diabetic atherosclerosis and renal dysfunction in streptozotocin-treated, apolipoprotein E-deficient mice. Physiol Rep 2014;2:e12043

19. Giacco F, Du X, D'Agati VD, et al. Knockdown of glyoxalase 1 mimics diabetic nephropathy in nondiabetic mice. Diabetes 2014;63:291–299

20. Vulesevic B, McNeill B, Geoffrion M, et al. Glyoxalase-1 overexpression in bone marrow cells reverses defective neovascularization in STZ-induced diabetic mice. Cardiovasc Res 2014;101:306–316

21. Molgat ASD, Tilokee EL, Rafatian G, et al. Hyperglycemia inhibits cardiac stem cell-mediated cardiac repair and angiogenic capacity. Circulation 2014;130(Suppl. 1):S70–S76

22. Yang YM, Huang A, Kaley G, Sun D. eNOS uncoupling and endothelial dysfunction in aged vessels. Am J Physiol Heart Circ Physiol 2009;297:H1829–H1836

23. Wang Y, Dakubo GD, Thurig S, Mazerolle CJ, Wallace VA. Retinal ganglion cell-derived sonic hedgehog locally controls proliferation and the timing of RGC development in the embryonic mouse retina. Development 2005;132:5103–5113

24. Cecchini MG, Felix R, Fleisch H, Cooper PH. Effect of bisphosphonates on proliferation and viability of mouse bone marrow-derived macrophages. J Bone Miner Res 1987;2:135–142

25. Hare JM, Stamler JS. NO/redox disequilibrium in the failing heart and cardiovascular system. J Clin Invest 2005;115:509–517

26. Odiete O, Hill MF, Sawyer DB. Neuregulin in cardiovascular development and disease. Circ Res 2012;111:1376–1385

27. Horstman LL, Jy W, Jimenez JJ, Ahn YS. Endothelial microparticles as markers of endothelial dysfunction. Front Biosci 2004;9:1118–1135

28. Hwang SJ, Ballantyne CM, Sharrett AR, et al. Circulating adhesion molecules VCAM-1, ICAM-1, and E-selectin in carotid atherosclerosis and incident coronary heart disease cases: the Atherosclerosis Risk In Communities (ARIC) study. Circulation 1997;96:4219–4225

29. Anker SD, von Haehling S. Inflammatory mediators in chronic heart failure: an overview. Heart 2004;90:464–470

30. Dalle-Donne I, Rossi R, Giustarini D, Milzani A, Colombo R. Protein carbonyl groups as biomarkers of oxidative stress. Clin Chim Acta 2003;329:23–38

31. Kageyama S, Yokoo H, Tomita K, et al. High glucose-induced apoptosis in human coronary artery endothelial cells involves up-regulation of death receptors. Cardiovasc Diabetol 2011;10:73

32. Baden T, Yamawaki H, Saito K, Mukohda M, Okada M, Hara Y. Telmisartan inhibits methylglyoxal-mediated cell death in human vascular endothelium. Biochem Biophys Res Commun 2008;373:253–257

33. Takahashi K, Tatsunami R, Oba T, Tampo Y. Buthionine sulfoximine promotes methylglyoxal-induced apoptotic cell death and oxidative stress in endothelial cells. Biol Pharm Bull 2010;33:556–560
34. Bento CF, Fernandes R, Matafome P, Sena C, Seiça R, Pereira P. Methylglyoxal-induced imbalance in the ratio of vascular endothelial growth factor to angiopoietin 2 secreted by retinal pigment epithelial cells leads to endothelial dysfunction. Exp Physiol 2010;95:955–970
35. Pentassuglia L, Sawyer DB. The role of Neuregulin-1beta/ErbB signaling in the heart. Exp Cell Res 2009;315:627–637
36. Gui C, Zhu L, Hu M, Lei L, Long Q. Neuregulin-1/ErbB signaling is impaired in the rat model of diabetic cardiomyopathy. Cardiovasc Pathol 2012;21:414–420
37. Ceradini DJ, Yao D, Grogan RH, et al. Decreasing intracellular superoxide corrects defective ischemia-induced new vessel formation in diabetic mice. J Biol Chem 2008;283:10930–10938
38. Jo-Watanabe A, Ohse T, Nishimatsu H, et al. Glyoxalase I reduces glycative and oxidative stress and prevents age-related endothelial dysfunction through modulation of endothelial nitric oxide synthase phosphorylation. Aging Cell 2014;13:519–528
39. Dinh W, Füth R, Nickl W, et al. Elevated plasma levels of TNF-alpha and interleukin-6 in patients with diastolic dysfunction and glucose metabolism disorders. Cardiovasc Diabetol 2009;8:58
40. Fan X, Subramaniam R, Weiss MF, Monnier VM. Methylglyoxal-bovine serum albumin stimulates tumor necrosis factor alpha secretion in RAW 264.7 cells through activation of mitogen-activating protein kinase, nuclear factor kappaB and intracellular reactive oxygen species formation. Arch Biochem Biophys 2003;409:274–286
41. Kleinbongard P, Heusch G, Schulz R. TNFalpha in atherosclerosis, myocardial ischemia/reperfusion and heart failure. Pharmacol Ther 2010;127:295–314
42. Chen Y, Pat B, Zheng J, et al. Tumor necrosis factor-alpha produced in cardiomyocytes mediates a predominant myocardial inflammatory response to stretch in early volume overload. J Mol Cell Cardiol 2010;49:70–78
43. Fiedler U, Reiss Y, Scharpfenecker M, et al. Angiopoietin-2 sensitizes endothelial cells to TNF-alpha and has a crucial role in the induction of inflammation. Nat Med 2006;12:235–239
44. Yao D, Taguchi T, Matsumura T, et al. High glucose increases angiopoietin-2 transcription in microvascular endothelial cells through methylglyoxal modification of mSin3A. J Biol Chem 2007;282:31038–31045
45. Xue J, Ray R, Singer D, et al. The receptor for advanced glycation end products (RAGE) specifically recognizes methylglyoxal-derived AGEs. Biochemistry 2014;53:3327–3335
46. Ramasamy R, Schmidt AM. Receptor for advanced glycation end products (RAGE) and implications for the pathophysiology of heart failure. Curr Heart Fail Rep 2012;9:107–116
47. Schmidt AM, Yan SD, Wautier JL, Stern D. Activation of receptor for advanced glycation end products: a mechanism for chronic vascular dysfunction in diabetic vasculopathy and atherosclerosis. Circ Res 1999;84:489–497
48. Brouwers O, de Vos-Houben JM, Niessen PM, et al. Mild oxidative damage in the diabetic rat heart is attenuated by glyoxalase-1 overexpression. Int J Mol Sci 2013;14:15724–15739
49. Yao D, Brownlee M. Hyperglycemia-induced reactive oxygen species increase expression of the receptor for advanced glycation end products (RAGE) and RAGE ligands. Diabetes 2010;59:249–255
50. Kehat I, Molkentin JD. Molecular pathways underlying cardiac remodeling during pathophysiological stimulation. Circulation 2010;122:2727–2735